Iraqi Geological Journal

Journal homepage: https://www.igj-iraq.org

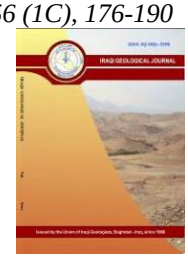

Multi-Sensor Remote Sensing Data and GIS Modeling for Mapping Groundwater Possibilities: A Case Study at the Western Side of Assiut Governorate, Egypt

Ezz El Deen S. Khattab[1,*], Hassan S. Sabet[1], Mostafa AbuBakr[1] and Taher M. Hassan[2]

[1] Department of Geology, Faculty of Science, Al-Azhar University, Cairo, Egypt

[2] National Water Research Centre, Research Institute for Groundwater, Cairo, Egypt

[*] **Correspondence**: ezzezz3939@yahoo.com

Received:
18 July 2022

Accepted:
10 November 2022

Published:
31 March 2023

Abstract

Groundwater is an essential natural resource and it has a significant role in the development of dry lands. It is the main source of fresh water in arid and semi-arid regions. The present study investigates groundwater potentiality in the western part of Assiut Governorate, Egypt using advanced remote sensing and geospatial techniques along with hydrological data and field validation. The adopted method provides a low-cost and highly effective tool that can be combined with the conventional land-based approach for mapping Groundwater Potentiality. The study aims to determine the groundwater probability and recharging zones based on the contribution of some physiographic variables that influence groundwater storage. Therefore, multi-sensors remote sensing data from ASTER, Landsat-8, MODIS, Shuttle Radar Topography Mission (SRTM), Tropical Rainfall Measuring Mission (TRMM), and Radarsat-1 were accustomed to extract several geospatial thematic layers (variables). These layers include elevation, slope, curvature, drainage density, topographic wetness index, surface roughness, frequency of thermal anomaly, accumulated precipitation, Land Use/Land Cover (LULC), and lineament density. The produced layers are then scaled and weighted based on their contributions to the recharge of near-surface (unconfined) groundwater aquifers through infiltration and percolation processes. The Simple Additive Weight (SAW) method was utilized to aggregate all the weighted layers for creating the Groundwater Potentiality map. This aggregated grouped map was then classified into 5 classes, from very high to very low groundwater potentiality zones. The results show that the high Groundwater Potentiality was associated with low terrain, high surface ruggedness, high drainage and lineament densities, and relatively close to thermal anomalies in wadi deposits, and adjacent sandy areas. The remote sensing results were validated using comprehensive field observations including, pumping tests, water wells data, and vegetation patterns in the study area. The study concluded that a groundwater possibility map based on geospatial techniques and remote sensing data can provide a robust tool in groundwater exploration, and consequently, it can be adopted elsewhere in arid regions.

Keywords: Ground water in west Assiut; GWP, Remote sensing; Geospatial techniques; Simple Additive Weight method (SAW)

DOI: 10.46717/igj.56.1C.12ms-2023-3-23

1. Introduction

In the last few decades, the water demands in Egypt is strongly increased due to the overpopulation and the ambition of reclamation projects all over the country (i.e., the New Valley, Toshka, New Delta, and the 1.5 million feddan El Salam reclamation projects) (Salem et al., 2016). In fact, groundwater has special importance due to the desert conditions prevailing in Egypt. With a limited share of water and deserts covering about 96% of the total area, Egypt relies on groundwater, which represents about 20% of the total potential water resources (Allam et al., 2003). Therefore, groundwater occurrence, assessment, management, and protection became significant and strategic task. Nowadays, the water shortage in Egypt pushes the government to invest and establish several water recycling projects, such as the saline water plants and wastewater management plants. These projects utilize the latest technology to produce/reuse fresh water from saline or wastewater, but this operation is expensive and consume huge amount of energy. According to the UN, Egypt has entered the water poverty area where the water per capita amounted is less than 500 m^3/year (Mahrous et al., 2016). Hence, the Egyptian government pays more attention to locate and define alternative renewable water resources, which would be the base for establishing new development and communities in Egypt. The study area locates in the western part of the Assiut Governorate and covers an area of about 635 km^2 in the arid zone, which is defined as hot and dry climatic conditions in the summer and temperature is low in the winter with rare rainfall.

Traditional techniques, such as geophysical tools, have been used successfully for mapping groundwater potentialities, especially in deserts (Elbeih et al., 2015). However, it is time and money consuming, complicated and only effective in local (small) areas. Therefore, the main goal of this study is to detect the high groundwater probability zones based on investigating the effect of physiographic and morphological features of sub-basins (catchments) that contribute positively in groundwater recharge and storage. Furthermore, field measurements were analyzed to validate the multi-sensor remote sensing data results to increase the confidence of the produced Groundwater Potential (GWP) map in the study area. The produced map can be used later as a supplemented tool with conventional geophysical methods. This relatively new technique was applied successfully in regions with similar climatic conditions (Amer et al., 2013; Elbeih, 2014; Abrams et al., 2018, and Zein El-Din et al., 2018).

The Relatively limited previous studies on the study area are summarized in the following .El Meligy (2004) classified the area of Assiut Governorate into four main hydrogeological provinces, each has its own geologic, hydrographic, and hydrologic characteristics; Eastern province includes the eastern plateau, southern province includes (Abu Tieg, Assiut), northern province extends widely from Assiut to Dayrout and east-Ibrahimia province in which the groundwater is directly recharged from the Ibrahimia Canal. Ahmed (2013) evaluated groundwater for drinking and domestic uses in Dayrout district and concluded that the TDS concentrations in groundwater at Dayrout district increased toward the desert fringe and decreased toward the floodplain areas. Moreover, Mahmod (2015) studied groundwater evaluation for drinking and domestic uses in Assiut Governorate, Egypt.

ElDakar et al. (2016) introduced a distribution map for the TDS concentration using GIS at Assiut, Egypt, and studied the interaction between surface water (SW) and groundwater (GW) and its impact on the groundwater salinity of quaternary aquifer in the area between Assiut and Dayrout, Egypt.

According to El Meligy (2004), the Eocene limestone aquifer is the primary aquifer in the region, which has a limited supply of water and is made up of fractured carbonate rocks of Samalut, Minia, and Drunka formations. This aquifer overlies the Nubia sandstone (Pre-Cenomanian) aquifer, the Quaternary and Plio-Pleistocene aquifers underlying this aquifer. It is a paleokarstified, low to moderately productive aquifer with minimal recharge from deep aquifers and surface runoff.

The salinity of the groundwater varies between 200 and 900 ppm, demonstrating the freshness of the water and this aquifer's groundwater depth is between 90 and 200 m, the transmissivity of the Eocene limestone aquifer ranges between 18.3 and 1758, This large fluctuation relates to the variation in voids

and fractures intensity. The Quaternary aquifer is situated on the study area's east edge and has a variety of compositions, from graded Pleistocene sand and gravel intercalated with clayey lenses taking up one area. Then comes the Plio-Pleistocene sand and clay intercalations with gravel encompassing an area with a width of 1-3 km at the edges (El Meligy, 2004). This aquifer's groundwater often has unconfined conditions (Said, 1962).

The current study will employ the powerful coverage of remote sensing data and geospatial technique to indirectly detect zones with high groundwater probabilities within the study area.

2. Study area

The study area is situated between latitudes 26°56′ 00″ and 27°19′ 00″ N and longitudes 30° 55′ 00″ and 31° 10′ 00″E (Fig. 1a).

The research area is a portion of the limestone plateau's reclaimed land, west of the governorate of Assiut. The region's development situation is greatly influenced by the geological setting. The types of rocks, the degree of porosity, Surface features, geologic structures, the composition of the sediment, the rarity of floods and the degrees of decline play a valuable role in the impact on the geo-environmental.

In essence, within the study area, the sedimentary sequence exposed consists of Quaternary rocks and sediments and Eocene. From bottom to top, the Eocene rocks are divided into two formations: Drunka and Minia (Fig. 1b).

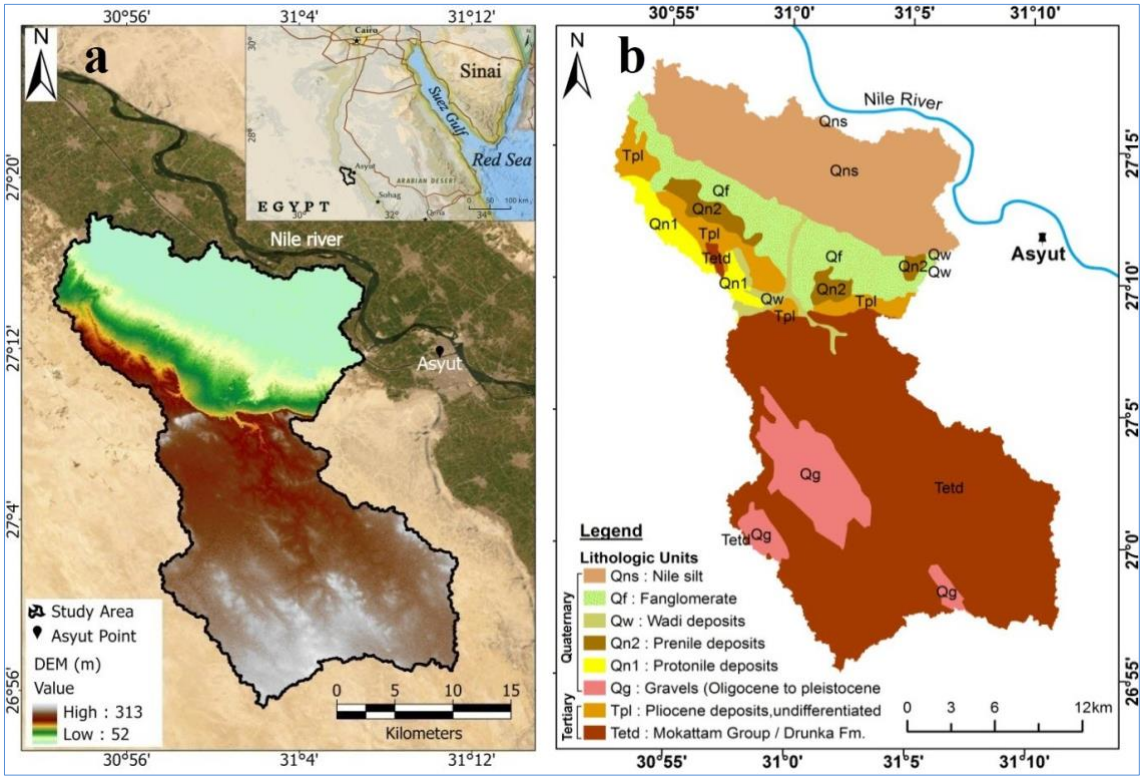

Fig. 1. A)Location map overlaid with topographical Digital Elevation Model (DEM) for the study area; B) Geologic map of the study area (modified after Conoco, 1987)

3. Data and Methodology

The study depends mainly on remote sensing data and GIS techniques with field validation, which can provide modern tools to determine sustainable groundwater resources for optimal uses. The remote sensing data included optical, radar and thermal satellite images for mapping GWP, especially in light of the scarcity of surface flow data in the study area.

To represent the physiographic impact on groundwater pools, the data types were selected an approved methodology was followed using the weighted index overlay analysis technique for computing the variable weights and producing the GWP map. These variables were extracted from remotely sensed data to make the proper integration between them to predict the shallow groundwater potential sites. The workflow for the utilized data and methods consists of two main procedures; first, variable extraction using the compiled remote sensing data products, and second, GWP analysis and modeling (Fig. 2).

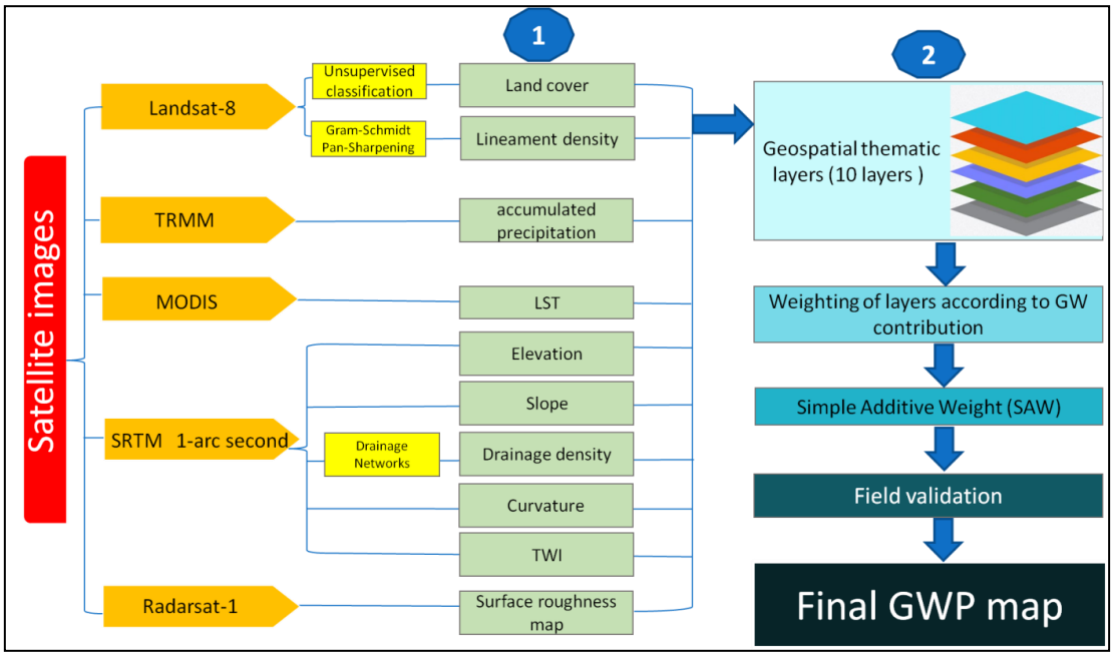

Fig. 2. Simplified work flow for the remote sensing data and the methodology; 1) Construction of thematic layers; 2) groundwater potentiality modeling.

3.1. Remote Sensing Data

Remote sensing technology has advanced to advanced levels of practicality, with regard to optical, radar, and thermal infrared images. Optical images can be used to map surface features, present land cover/use, and vegetation distribution patterns in addition to lithological details of the study area. On the other hand, space borne radar images are a powerful tool in mapping surface roughness and characteristics of rivers buried in sand, such as ancient river beds and lake basins, e.g., Mccauley et al., 1982; Ghoneim and El-Baz, 2007; and AbuBakr et al., 2013. In addition, the Shuttle Radar Topography Mission (SRTM) is the most common source of the Digital Elevation Model (DEM) and is strong in fixing surface drainage networks (e.g., Ghoneim et al., 2007). Thermal infrared (TIR) can be used to track the accumulations of moisture content near the surface after precipitation events, especially in sandy deserts (e.g., Ghoneim, 2008), Like the area under investigation.

In this study, optical, radar and thermal data were utilized, including (ALOS PALSAR DEM 12.5 m), Operational Land Imager (OLI), Moderate Resolution Imaging Spectroradiometer (MODIS), Shuttle Radar Topography Mission (SRTM), Tropical Rainfall Measuring Mission (TRMM), and Radarsat-1. These wide set of data were downloaded from the USGS and NASA's websites, which are open sources (Table 1).

Table1. Remote sensing data description, sources and associated layers.

Sensor	Source	Data	Spatial Resolution	Generated Thematic Layer
Shuttle Radar Topography Mission (SRTM)	USGS Earth Explorer [https://earthexplorer.usgs.gov/]	Digital Elevation Model (DEM)	30m	Elevation, Slope, Curvature, Drainage Density, Topographic Wetness Index
Advanced Spaceborne Thermal Emmision ReVection Radiometer (ASTER)	USGS Earth Explorer [https://earthexplorer.usgs.gov/]	Level 1T Multispectral Imagery	15m VNIR, 30m MIR, 90m TIR	Landcover
Tropical Rainfal Measuring Mission (TRMM)	Nasa Giovanni https://giovanni.gsfc.nasa.gov/giovanni/	Radar Precipitation Measurements	1/4th Degree (27km)	Accumulated Precipitation
Moderate Resolution Imaging Spectroradiometer (MODIS)	USGS Earth Explorer [https://earthexplorer.usgs.gov/]	Daily Daytime Land Surface Temperature	1km	Land Surface Temperature
Landsat-8 Operational Land Imager	USGS Earth Explorer [https://earthexplorer.usgs.gov/]	Multispectral Imagery	30m	Landcover, Lineament Density
Radarsat-1	The Center for Remote Sensing in Boston University	C-band Radar, HH Polarization	12.5m	Surface Roughness

3.2. Methodology

According to the workflow in Fig. 2, the adopted methodology was divided into two main parts, first building the required thematic layers and second, applying the modeling techniques to detect groundwater Potentiality.

3.2.1. Building the required thematic layers

We have created ten thematic layers (variants), which are mainly extracted from satellite data. These layers are elevation, slope, curvature, drainage density, Topographic Wetness Index (TWI), surface roughness, frequency of thermal anomaly, accumulated precipitation, Land Use / Land Cover (LULC) and lineament density. These variables will be mentioned in detail in the following sections, based on their data sources.

- Elevation and DEM derived layers

The Digital Elevation Model (DEM) data were created by mosaicking two tiles of SRTM1Arc-Second (30 m), and then this mosaic was cropped to match the boundary of the study area. The spatial analyst tools in ArcGIS10.5 were used to produce the slope, standard curvature, and drainage density layers (Fig. 3a, b, c and d).

The slope and curvature provide an explanation of the infiltration conditions in water catchments (basins). The slope measures the change of relief per degree (raster unit) and thus measures the runoff acceleration from upstream to downstream. The slope (degrees) layer was derived from the DEM using the surface tools in ArcGIS. The SRTM-DEM was also used to produce the standard curvature layer, which gives an interpretation to the concavity and convexity of the ground surface as positive and negative values, respectively.

According to Jenson and Dominque (1988), the surface flow direction was computed using the eight directions model (D3), then the flow accumulation was calculated, and the drainage network was determined using a threshold at 300. Ultimately, a density map was extracted based on the produced drainage patterns and calculated in a square kilometers.

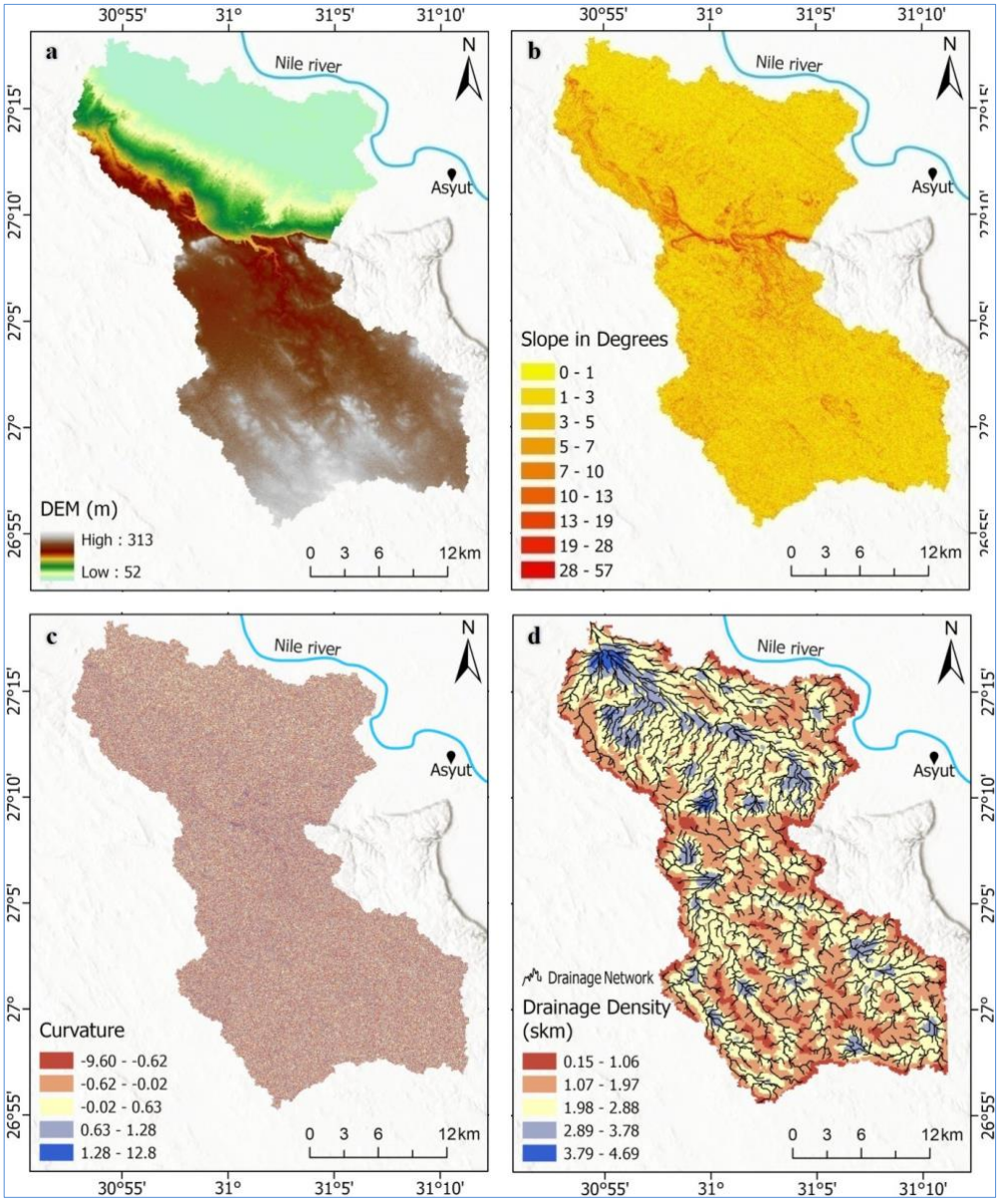

Fig. 3. Elevation and DEM derived layers; **a.** Elevation, **b.** Slope, **c**. Curvature, **d.** Drainage Density.

- Topographic wetness index (TWI)

The Topographic Wetness Index (TWI) was developed by Beven and Kirkby (1979) to expresse the steady state of wetness, which is usually applied to quantify the topographic control on hydrological processes (Sørensen et al., 2006, Abrams et al., 2018). TWI is usually applied to assess the effect of topography and soil moisture depending on the formerly created slope and flow accumulation layers. The TWI layer was calculated using the following equation:

$$\ln (a/ \tan b) \quad (1)$$

Where, a is the upslope area of a given cell and b is the slope in radians. Using the above equation the TWI was created in the raster calculator tool in ArcGIS software (Fig. 4a).

- Surface roughness

According to Gaber et al., 2011, Surface Roughness (SR) can be extracted based on radar back scattering waves, which has a strong effect on microwave signals. According to Lee and Pottier, 2009, the L-band with its longer wavelength has more penetration depth and could be less sensitive to slight changes in wadi surface roughness (micro-roughness) than the microwave with shorter wavelength of

C-band. Therefore, Radarsat-1 satellite images (C-band) were used to create the surface roughness map of the study area to classify the texture of surface sediments into five classes: very rough, rough, medium, fine, and very fine materials (Fig. 4b).

- Land surface temperature (LST)

According to AbuBakr, 2014, Monitoring thermal change in the bare sandy surface after precipitation can provide indirect indications of groundwater accumulations. We used thermal remote sensing data here to identify and examine thermal anomalies in the study area to identify possible surface groundwater infiltration zones. In other meaning, it tries to uncover the possible link between these anomalies and groundwater leakage. This method was used successfully to detect groundwater in similar arid lands, such as the North Sinai Peninsula and the United Arab Emirates (AbuBakr, 2014; Ghoneim, 2008).

A systematic analysis for thermal infrared (TIR) data of daily MODIS LST were extracted from the MODIS MYD11A1 V6 image, which provides per-pixel land surface temperature (LST) in a 1200 x 1200 kilometer grid (Wan et al., 2015). MODIS tiles were re-projected from their original Sinusoidal (ISIN) projection to UTM-36N projection and then combined and clipped to the study area boundary, and finally the pixel values were converted from Kelvin to Celsius degrees (Fig. 4c).

- Accumulated Precipitation

Due to the lack of rainfall monitoring stations in the study area, the Tropical Rainfall Measuring Mission (TRMM) was used to estimate the accumulated precipitation. TRMM is a joint space mission between NASA and Japan Aerospace Exploration Agency (JAXA) designed to monitor and study tropical rainfall. This mission provides global rainfall data with a 0.25° × 0.25° footprint since 1997. Despite the coarse resolution of the satellite rainfall products, they are used in a wide range of applications due to their being cost effective and available for the globe (Harris et al., 2007). Thus, TRMM was employed here to estimate the amount of rainfall events that were occurred between 2012 and 2018.

The precipitation data was extracted using TRMM 3B43 V7 for 6 years (from 2012 to2018). The TRMM data were converted from net cdf format to vector points then an interpolation process was applied using spline method to convert back the point vectors to interpolated raster, which was then clipped and adjusted to the extent of the investigated area (Fig. 4d).

- Land use/land cover (LULC)

The LULC is significant for mapping the variation in soil types and anthropogenic activities in the plain area, which is critical for runoff infiltration. These layers were produced from the OLI sensor, which was mounted on the Landsat-8. Several pre-processing analyses were applied, including atmospheric correction, which removes the effects of the atmosphere (scattering and absorption) and the DN was ultimately converted to surface radiance. After that, a Principal Component Analysis (PCA) was carried out as an image transformation technique to enhance the spectral resolution of the images to reduce the redundancy of the data before going through the image classification (Lillesand & Kiefer, 1987). Another step was performed prior image classification, which is the extraction and masking the vegetation in the study area through applying the Normalized Difference Vegetation Index (NDVI) (Weier and Herring, 2000). The resulted vegetation vector layer is compared with the OLI image using a false band combination (bands 5, 4, 3 in RGB, respectively) as a verification step before proceeding to the classification process.

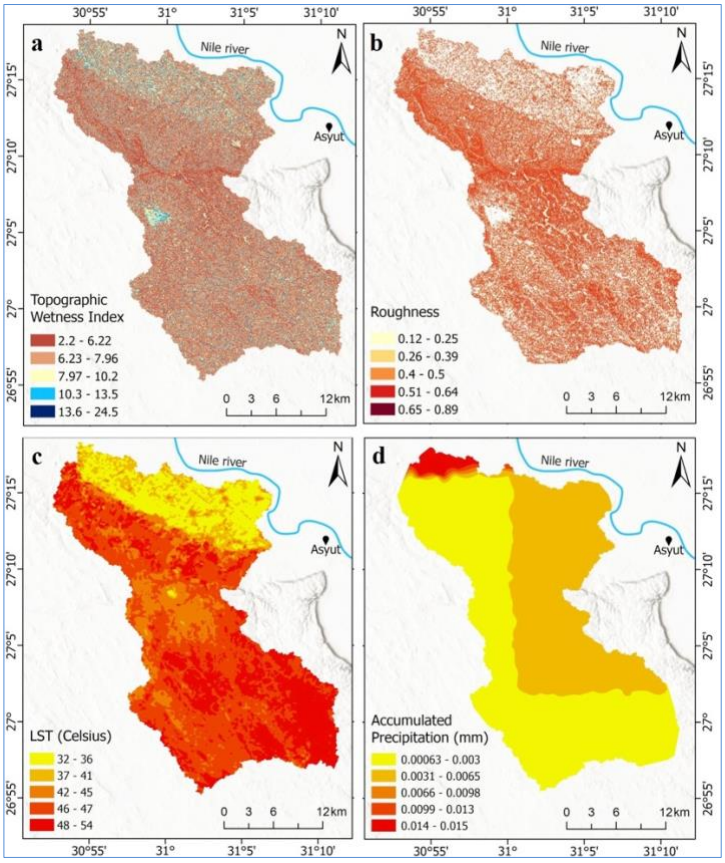

Fig. 4. A)Topographic wetness Index; B) Surface roughness; C) Land surface temperature; D) Accumulated precipitation

A K-Means classification method was adopted to classify the land cover in the study area. The technical classification parameters were comprised of a threshold of 5%, and maximum iterations of 50 to produce 20 classes. The spectrally similar classes were merged together according to the surface lithology and the type of land use with the aid of the published geological map (EGSMA, 1994) and high resolution imagery in Google Earth. The final product involved 5 classes of LULC: basement rocks, old alluvial deposits, recent and wadi deposits, sedimentary rocks, urban, roads and vegetation (Fig. 5a).

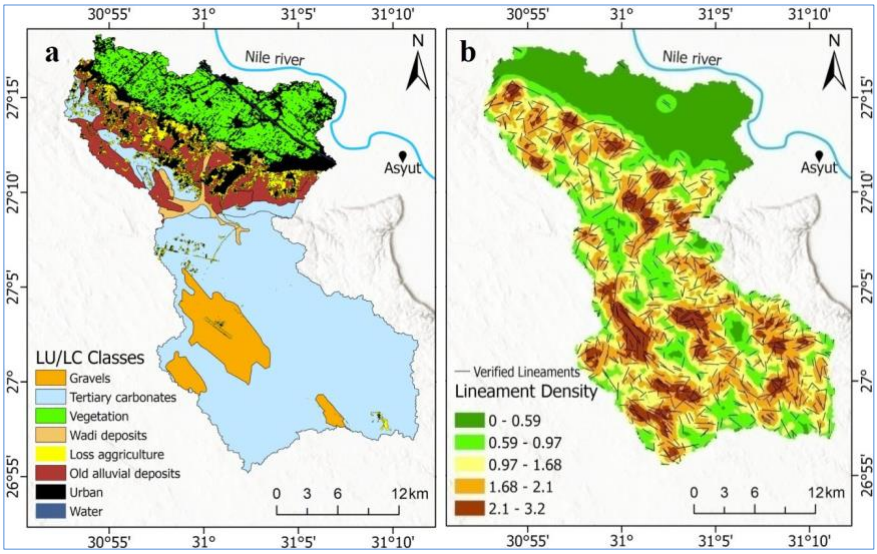

Fig. 5. A) Land use/land cover (LU\LC); B) Lineament density

- Lineament density

According to (Smith and Wise, 2007) the precision of lineament extraction from optical satellite images relied on sensor characteristics, spatial and immaterial separation, and weather board-brightness qualification. Therefore, lineaments were extracted from theLandsat-8imagesafter applying the Gram-Schmidt transformation to enhance the spatial resolution of the multispectral OLI image (Laben and Brower, 2000). The are lineaments then exported to Google Earth software for usage to validate them and remove false lineaments, such as roads, trail, and other manmade activities. Ultimately, the lineaments with high degree of confidant were selected and a line density layer was created using the same procedure groove of the drainage density layer (Fig. 5b).

3.2.2. Groundwater potentiality indexing and modelling

It is pointless to perform groundwater potentiality modeling directly on the extracted thematic layers without a weighted index connecting them together based on their groundwater contribution. Therefore, a semiquantitative weighted index (GWP indexing) was used to divide each thematic layer into only 5 classes.

- Semi-Quantitative Weighted Index

This index was selected based on previous studies on regions with similar conditions (e.g., AbuBakr et al., 2013; Abrams et al., 2018). Furthermore, field investigations in the study area and literature review significantly contributed to the assignment of the GWP indexing.

The layers were approximately changeless and classified into five classes using the natural break (Jenks) method (Jenks, 1967), to increase the resolution across the study area (Table 2).

Each class was assigned to a common scale value, which could frequent from 0 to 100 as a value of contribution in the GWP for propagate the conclusive formula of the thematic layers (Figs. 6, 7 and 8). Larger scale value indicative to higher GWP and imperfection versa. For token, the very supercilious height and steep slope represent very low contribution (0-20) in GWP, while very low elevation and bland sloping contemplate very high to high contribution (80-100) in GWP (Table 2).

Table 2. All variables and weights according to contribution to GW

weight variables	**20**	**40**	**60**	**80**	**100**
Elevation (m)	v. high 254–313	High 218–254	medium 160–218	low 95–160	v. low 52–95
Slope (degree)	v. high 37–57	High 27–37	medium 17–27	low 7–17	v. low 0–7
Curvature	v. low -9.6–-0.62	Low -0.62–-0.02	medium -0.02–0.63	high 0.63–1.28	v. high 1.28–12.8
Drainage density	v. low 0.15–1.06	Low 1.06–1.97	medium 1.97–2.88	high 2.88–3.78	v. high 3.78–4.69
TWI	v. low 2.2 –7	Low 7 – 9	medium 9 –11	high 11– 20	v. high 20 – 25
Surface Roughness	v. soft	Soft	medium	rough	v. rough
LST (C)	v. high 47–54	High 42–47	medium 37–42	low 35–37	v. low 31–35
Acc. Precipitation	v. low 0.00062–0.0065	Low 0.0065–0.0098	medium 0.0098–0.0099	high 0.0099–0.014	v. high 0.014–0.015
LULC	Urban & Roads	Sed. Rocks	Tertiary Deposits	Quaternary deposits	Vegetation
Lineament Density	v. low 0 – 0.46	Low 0.46– 1.01	medium 1.01 – 1.34	high 1.34 – 1.64	v. high 1.64– 2.41

- Simple additive weight method (SAW)

There are several techniques of GWP overlay modelling, most of them have been standard and estimated, such as Probabilistic Frequency Ratios (PFR) (Manap et al., 2013; Naghibi et al., 2015), the Analytical Hierarchy Process (AHP) (Adiat et al., 2012; Mallick et al., 2015), and the Simple Additive Weight (SAW) (Abrams et al., 2018; Al-Ruzouq et al., 2015).

According to these studies, especially Abrams et al., (2018), the Simple Additive Weight method (SAW) is one of the effective methods for modeling groundwater potential. The SAW technique is the most primitive of the semiquantitative index-overlay techniques. It assigns equal weight to all variables (layers) and assumes that the assigned GWP values are adequate to represent potentiality (Abrams et al., 2018).

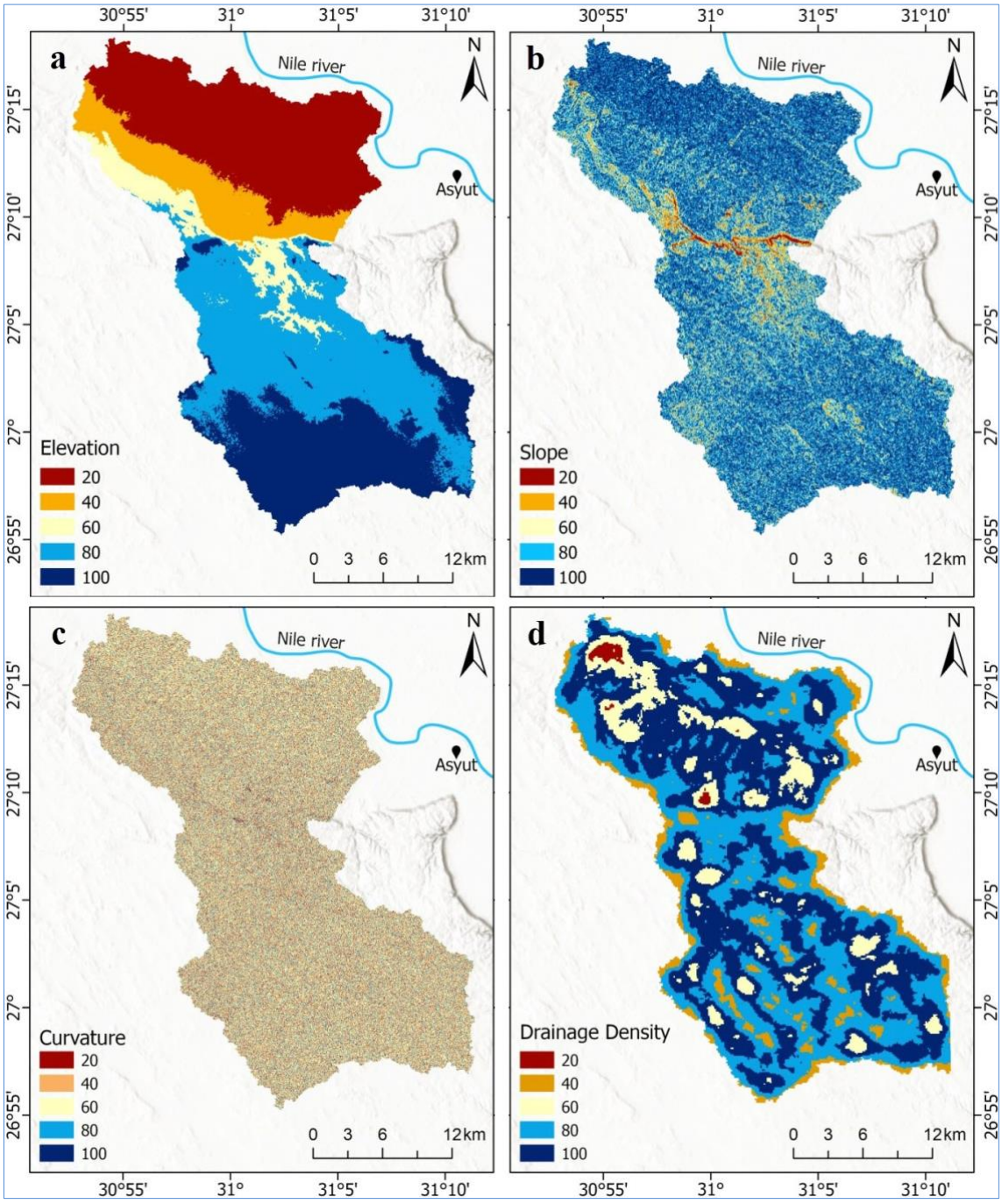

Fig. 6. A)Elevation weight; B) Slope weight; C) Curvature weight; D) Drainage Density weight

Therefore the 10 weighted thematic layers were summed together using the following SAW formula:

$$GWP_{SAW} = \sum GWP_E, GWP_S, GWP_{DD}, GWP_{LD}, GWP_C, GWP_{LC}, GWP_{SR}, GWP_{LST}, GWP_{TWI}, GWP_{AP} \quad (2)$$

Where, GWP_S, is the SAW technique for all groundwater potential, GWP_E potential for elevation, GWP_S potential for slope, GWP_{DD} potential for drainage density, GWP_{LD} potential for lineament density, GWP_C potential for curvature, GWP_{LC} potential for land cover, GWP_{SR} potential for surface roughness, GWP_{LST} potential for land surface temperature, GWP_{TWI} potentialfor topographic wetness index and GWP_{AP} is the potential for accumulated precipitation.

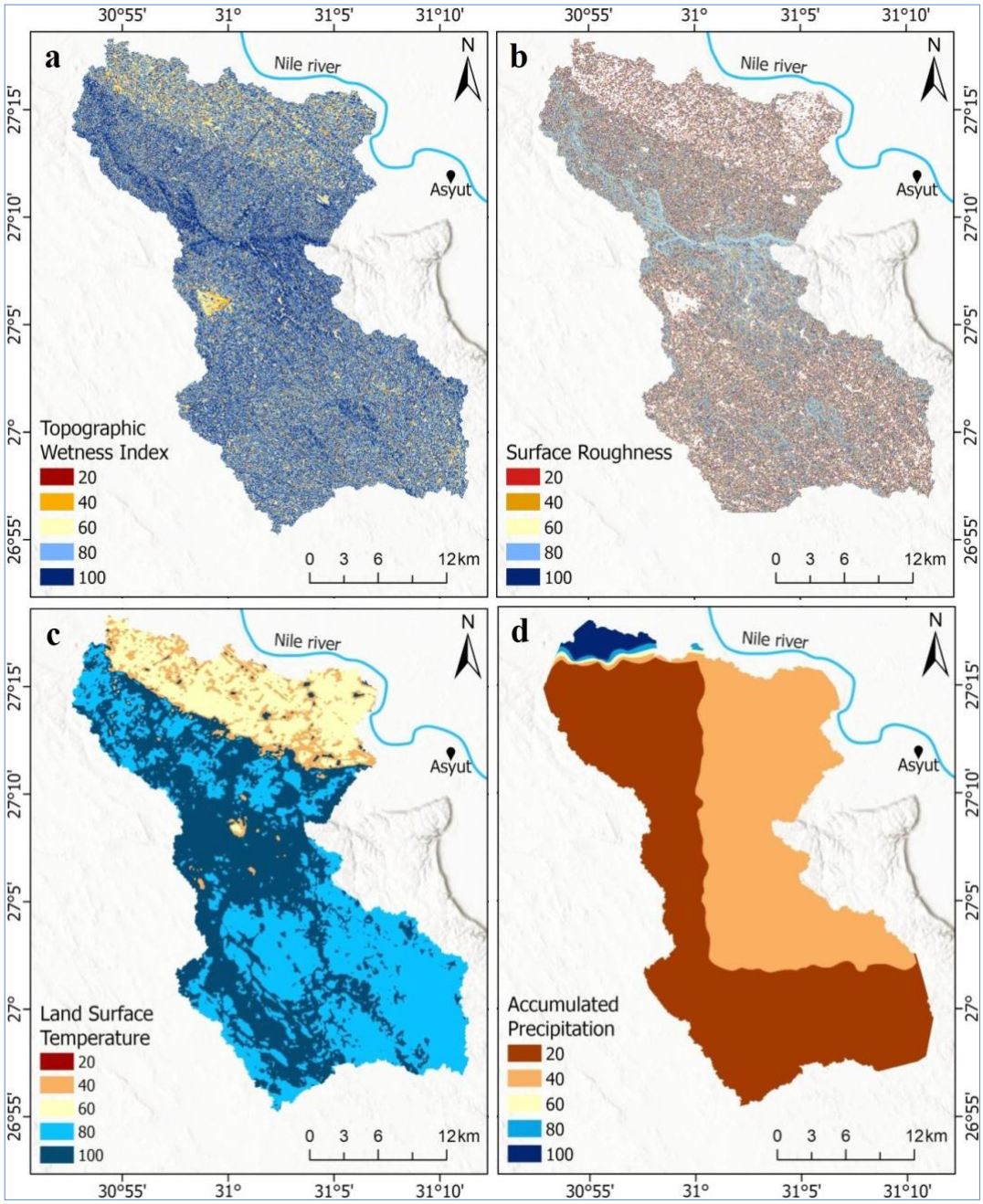

Fig. 7. A)Topographic Wetness Index weight,; B)Surface roughness weight; C) LST weight; D) Accumulated precipitation weight

4. Result and Discussion

The produced GWP map, based on the SAW overlay modeling, was classified into 5 main zones that reflect the possibility of groundwater potentiality: very high (73- 84), high (62-73), medium (51-62), low (40-51) and very low (30-40) (Fig. 9).

The interpretation of the GWP map reveals that most of the very high (VH) zone was defined along the north side of the study area. In other words, the very high GWP zone is extended along the cultivated land at the western bank of the Nile River. The extension of this zone is reasonable and can be attributed to the massive runoff that originates from the southern part and flows toward the northern part, where the flow velocity slows down due to the gentle slope and provides optimum conditions for the infiltration process.

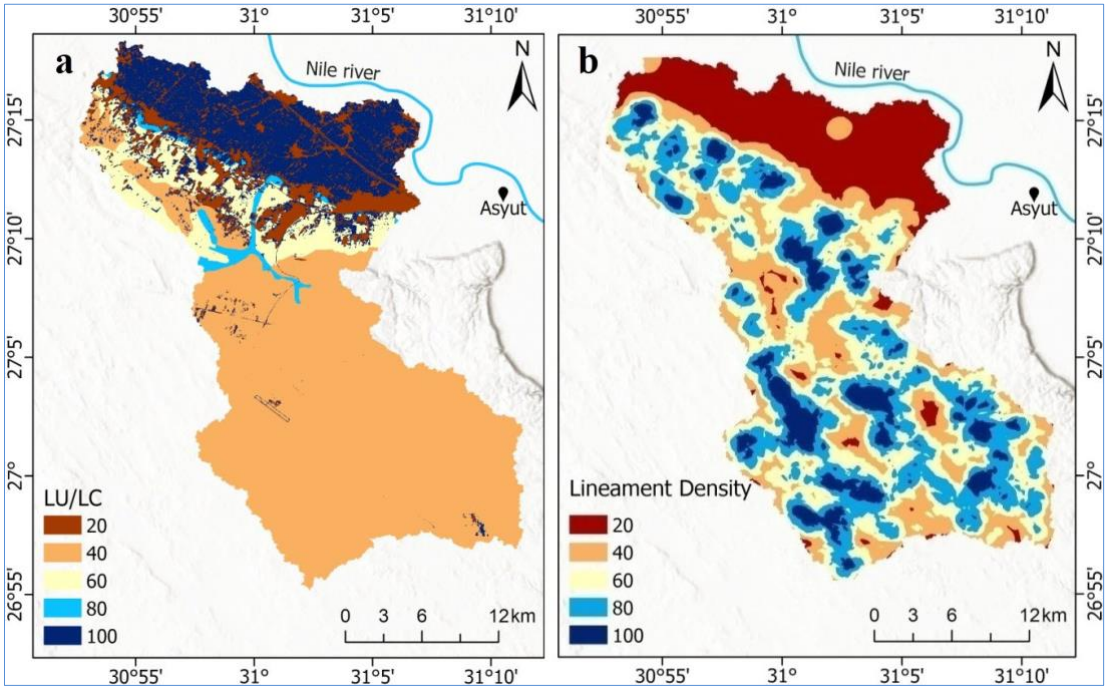

Fig. 8. A) LU\LC weight; B)Lineament density weight

On the other hand, the high (H) GWP zone is distributed in regions with high lineament density and surface roughness. The Moderate (M) zone occupies a relatively smaller portion of the plain. The low and very low (L and VL) zones are predominately in the southern part of the study area due to the steep slope and low infiltration conditions. These outcomes conclude that the VH and H GWP were generally associated with low terrain, high surface ruggedness, dense drainage, and lineament, relatively close to thermal anomalies, and fluvial wadi deposits or sandy areas.

4.1. Field Validation

The fieldwork of the present study was carried out in April, 2018 to confirm the remote sensing data results and the accuracy of the GWP map (Fig. 9), which included several confined pumping and recovery tests.

Fieldwork also included projections of some well locations on the final GWP map to validate model assumptions for the five different GWP zones (Fig. 9). The results showed that 100% of the wells were located in the high GWP zone. Most of these wells were drilled according to geophysical surveys (mainly geo-resistivity), which produced good water quality for industrial and agricultural purposes. Therefore, based on the distribution of the investigated wells in the study area, the overall accuracy of

the GWP is roughly estimated to be around 81%. However, further geophysical studies of the delineated VH and H GWP belts in the study area are recommended.

5. Conclusions

This study integrates remote sensing data and geospatial techniques for mapping groundwater potential in one of the most promising locations for development in Upper Egypt. The significance of utilizing remote sensing data instead of conventional land-based techniques came to produce a continuous surface map with higher resolutions and consistent scales than previously published maps, and to overcome the scarce of surface flow data. The key objective of this work was identifying physiographic variables that affecting groundwater recharge and storage for detecting renewable ground water accumulation.

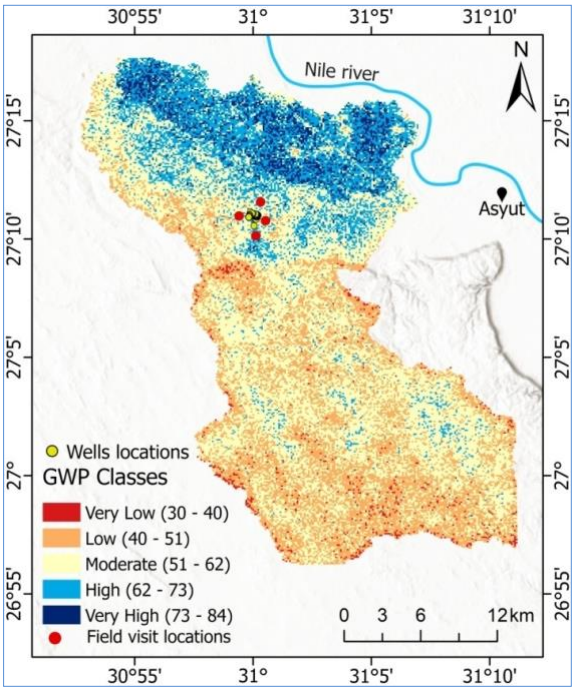

Fig. 9. Groundwater potential map with locations of field verification sites

A huge variety of remote sensing data, which includes optical, radar, and thermal sensors have been used to assemble numerous geospatial thematic layers (variables). These variables consist of elevation, slope, curvature, drainage density, topographic wetness index, floor roughness, frequency of thermal anomaly, gathered precipitation, Land Use/Land Cover (LULC) and lineament density. All variables have been organized and weighted primarily based on their contributions in groundwater recharge via infiltration and percolation processes. The Simple Additive Weight (SAW) technique turned into followed for computing the variable weights and generating the GWP map.

Fieldwork was conducted along the study area to validate the remote sensing data results and the accuracy of the produced GWP map through pumping test, collecting water well samples, mapping farms and other vegetation patterns in the study area. The fieldwork shows that most of the water wells are located in the high GWP zones, Therefore, the general accuracy of the produced GWP changed into the kind of anticipated at approximately 81%. However, for vital discipline validation to the result, geophysical investigations need to be performed on the provided VH and H GWP zones. In conclusion, the existing provides a geospatial-based tool to define zones with excessive groundwater opportunity for downscaling the exploration efforts via traditional land-primarily based totally techniques and might be carried out somewhere else in arid regions.

References

Abrams, W., Ghoneim, E., Shew, R., La Maskin, T., Al-Bloushi, K., Hussein, S., El-Baz, F., 2018. Delineation of groundwater potential (GWP) in the northern United Arab Emirates and Oman using geospatial technologies in conjunction with Simple Additive Weight (SAW), Analytical Hierarchy Process (AHP), and Probabilistic Frequency Ratio(PFR) techniques. Journal of Arid Environments, 157, 77–96.

AbuBakr, M. ,2014. Hydrological Modeling by Remote Sensing, GIS and Subsurface Geological Data Integration For Groundwater Exploration and Flash Flood Estimation in Northern Sinai. Al-Azhar University and Boston University.

AbuBakr, M., Ghoneim, E., El-Baz, F., Zeneldin, M.,& Zeid, S. 2013.Use of radar data to unveil the paleolake sand the ancestral course of Wadi El-Arish, Sinai Peninsula, Egypt. Geomorphology,194,34–45.

Adiat, K.A.N., Nawawi, M.N.M., Abdullah, K., 2012. Assessing the accuracy of GIS-based elementary multicriteria decision analysis as a spatial prediction tool – A case of predicting potential zones of sustainable groundwater resources. Journal of Hydrology, 440–441,75–89.

Ahmed, R.A.A., 2013. Groundwater Evaluation for Drinking and Domestic Uses in Diruot Distict, Egypt. M.Sc. Thesis, Assiut University.

Al-Ruzouq, R., Shanableh, A., Merabtene, T., 2015. Geomatics for Mapping of Groundwater Potential Zones in Northern Part of the United Arab Emiratis-Sharjah City. ISPRS-International Archives of the Photogrammetry, Remote Sensing and Spatial Information Sciences, XL-7/W3, 581–586.

Allam, A.R., Saaf, E. and Dawoud, M.A., 2003. Desalination of brackish groundwater in Egypt. Desalination, 152, 19-26

Amer, R., Sultan, M., Ripperdan, R., Ghulam, A., Kusky, T., 2013. An integrated approach for groundwater potential zoning in shallow fracture zone aquifers. International Journal of Remote Sensing, 34(19), 6539–6561.

Beven, K.J., Kirkby, M.J., 1979. Aphysically based, variable contributing are a model of basin hydrology. Hydrological Sciences Bulletin.

Egyptian Mineral Resources General Authority, E., 1994. Geological map of Sinai, sheetno1, scale 1:250000. Cairo.

El Dakar M.A., 2016. Surface Water- Grounedwater Interaction and its Impact on the Groundwater Salinity of the Quaternary Aqufer at the area west of the nile, between Assiut and Dayrout, EGYPT. M.Sc. Thesis: Assiut University, Egypt.

El Meligy, E.M., 2004. Groundwater Resources Evaluation of Assiut Area. Ph.D. Thesis, Faculity of Science, Assiut University, Egypt.

Elbeih, S.F., 2015. An overview of integrated remote sensing and GIS for groundwater mapping in Egypt. Ain Shams Engineering Journal, 6(1), 1–15.

Gaber, A., Koch, M., Griesh, M.H., Sato, M., 2011. SAR remote sensing of buried faults: Implications for groundwater exploration in the western desert of Egypt. Sensing and Imaging, 12(3–4), 133–151.

Ghoneim, E., 2008. Optimum groundwater locations in the northern United Arab Emirates. International Journal of Remote Sensing, 29(20), 5879–5906.

Ghoneim, E., El-Baz, F.,2007.The application of radar topographic data to mapping mega-paleodrainage in the Eastern Sahara. Journal of Arid Environments.

Jenks, G.F., 1967. The Data Model Concept in Statistical Mapping. International Year book of Cartography, 8241517

Jenson, S.K., Dominque, J.O., Domingue, J.O., 1988. Extracting Topographic Structure from Digital Elevation Data for Geographic Information System Analysis. Engineering, 54(11), 1593–1600.

Laben, C.A., Brower, B.V., 2000. Process for Enhancing the Spatial Resolution of Multispectral Imagery Using Pan-Sharpening. Google Patents.

Lee, J.S., Pottier, E., 2009. Polarimetric radar imaging: From basics to applications. Polarimetric Radar Imaging: From Basics to Applications. CRC Press.

Lillesand, T.M., Kiefer, R.W., 1987. Remote Sensing and Image Interpretation (2nd ed.). Wiley, NewYork.

Mahmod, O.A.E., 2015. Groundwater Evaluation for Drinking and Domestic Uses in Assiut Governorate, Egypt. M.Sc. Thesis, Assiut University, Egypt.

Mahrous, H.M., Bahgaat, W.K., 2019. Research Article Efficiency of Water Resources in Small and Medium-sized Dairy Factories in Egypt. International Journal of Dairy Science, 14(1), 1-11.

Mallick, J., Singh, C.K., Al-Wadi, H., Ahmed, M., Rahman, A., Shashtri, S., Mukherjee, S., 2015. Geospatial and geostatistical approach for groundwater potential zone delineation. Hydrological Processes, 29(3), 395–418.

Manap, M.A., Sulaiman, W.N.A., Ramli, M.F., Pradhan, B., Surip, N., 2013. A knowledge-driven GIS modeling technique for groundwater potential mapping at the Upper Langat Basin, Malaysia. Arabian Journal of Geosciences, 6(5), 1621–1637.

Mccauley, J.F., Schaber, G.G., Breed, C.S., Grolier, M.J., Haynes, C.V., Issawi, B., Elachi, C., Blom, R., 1982. Subsurface valley sand geoarcheology of the Eastern Sahara revealed by shuttle radar. Science, 218(4576), 1004-1020.

Naghibi, S.A., Pourghasemi, H.R., Pourtaghi, Z. S., Rezaei, A., 2015. Groundwater qanat potential mapping using frequency ratio and Shannon' sentropy models in the Moghan watershed, Iran. Earth Science Informatics, 8(1), 171–186.

Said, R., 1962. The Geology of Egypt. Elsevier Pub. Co., Amsterdam, New York .

Salem, M., Osman, T., 2016. A new map for urban development in Egypt, depending on mega projects of renewable energy. In Sustainable Mega Projects Conference, At British University in Egypt (Vol. 2).

Smith, M.J., Wise, S.M., 2007. Problems of bias in mapping linear landforms from satellite imagery. International Journal of Applied Earth Observation and Geoinformation, 9(1), 65-78.

Sørensen, R., Zinko, U., Seibert, J., 2006. On the calculation of the topographic wetness index: Evaluation of different methods based on field observations. Hydrology and Earth System Sciences, 10(1), 101–112.

Wan, Z., Hook, S., Hulley, G., 2015. MYD11A1 MODIS/Aqua Land Surface Temperature/ Emissivity Daily L3 Global1km SIN Grid V006 [Dataset]. NASA EOSDISLPDAAC.

Weier, J., Herring, D., 2000. Measuring Vegetation (NDVI & EVI). NASA Earth Observatory, Washington DC.